

# Mathematical Model of the RRR Anthropomorphic Mechanism for 2D Biomechanical Analysis of a Deep Squat and Related Forms of Movement

Václav Bittner<sup>1,2</sup>, Radim Štrýncl<sup>2</sup>, Karel Jelen<sup>2</sup>, Martin Svoboda<sup>3</sup>

<sup>1</sup>Faculty of Science, Humanities and Education, Technical University of Liberec, Studentská 2, Liberec, Czech Republic, E-mail: vaclav.bittner@tul.cz

<sup>2</sup>Faculty of Physical Education and Sport, Charles University in Prague, José Martího 31, Praha 6, Czech Republic, E-mail: jelen@ftvs.cuni.cz, radimstrync1@seznam.cz

<sup>3</sup>Faculty of Mechanical Engineering, Jan Evangelista Purkyně University in Ústí nad Labem, Pasteurova 1, Ústí nad Labem, Czech Republic

E-mail: martin.svoboda@ujep.cz

The aim of this study was to create a mathematical model of the RRR anthropomorphic mechanism for a 2D biomechanical analysis of a deep squat and related forms of movement. The segment stick model is designed to diagnose the movement with sagittal plan symmetry. Based on the input data from kinematic and dynamometric analysis, and from the anthropometric data of the monitored person, it is possible to estimate the resulting momentum of the forces acting on the main joints of the lower body. The technology may be applied in analysing deep squats, studying the dynamics of vertical reflection as well as in the biomechanical analysis of related forms of movement (e.g. standing-up, squatting with a dumbbell, skiing in downhill posture, etc.). The derived motion equations may be used to analyse the dynamics of the movement of anthropomorphic or mechatronic systems with the same geometry.

**Keywords:** Mathematical model, RRR mechatronic system, anthropomorphic mechanism, biomechanical analysis of movement

## 1 Introduction

One of the most topical biomechanical issues of today is the deep squat. It represents the basic movement model of primates and ranks among their natural postural positions. It is a posture where the flexion in the knee joint enables the back of the thighs to touch the calves, the heels stay on the ground and the spine is upright in a neutral position. This posture may be seen in young children. Based on an innate movement model, they instinctively use a deep squat if they want to reach the ground with their hand. They also play in this posture.

Practical experience shows that the majority of the Euro-Atlantic population in developed countries is losing the ability to reach the bottom position of a deep squat, or they are not using this movement pattern at all. However, studies proving the positive effect of the deep squat on the production of muscle power production and the performance of lower limbs may be found in world literature [1], [2], [3], [4]. Doubts regarding the overstraining of the knee joints are then disproved by Bryanton [2]. He found out that together with the engagement of the glutei, it is mainly the load of the hip joints that increases with the depth of a squat, not the knee joints.

Most studies on the deep squat are based on a kinesio-

logic analysis and the combination of a kinematic analysis with EMG. These methods cannot be used for objective conclusions on the momentum of the forces acting on particular joints during the respective stages of a deep squat. Therefore, the aim of this study is to create a model of an anthropomorphic mechanism that would enable such a biomechanical analysis of a deep squat and related forms of movements. The study focuses on the diagnosis of movement in the sagittal plane.

## 2 Segment structure and parametrization of the model

The model is created to diagnose the lateral movement projection of a person with the permanent support of both feet. It is based on a 3-segment 3D stick anthropomorphic mechanism when the feet, shins and shanks of both limbs are aligned, see Fig. 1. To derive motion equations, the weight of shank  $m_s$ , thigh  $m_t$  and half the weight of the upper body (head -  $h$ , upper limbs -  $a$ , trunk -  $r$ ) is respected as a unit  $m_b$  due to the symmetry. The weights and respective moments of inertia ( $I_s$ ,  $I_t$ ,  $I_b$ ) of particular segments may be estimated based on the method of Zatsiorsky et al. [5] from the body height ( $v$  [cm]) and total weight ( $m$  [kg]) of a person according to the equations (1).

$$\begin{aligned} m_\alpha &= E_{\alpha 0} + E_{\alpha 1}m + E_{\alpha 2}v, & [kg]; \\ I_\alpha &= m_\alpha k_\alpha^2 + F_{\alpha 0} + F_{\alpha 1}m + F_{\alpha 2}v, & [kg \cdot m^2]; \quad \alpha \in \{s, t\}; \\ m_\beta &= \sum_\beta (E_{\beta 0} + E_{\beta 1}m + E_{\beta 2}v), & [kg]; \\ m_b &= \sum_\beta m_\beta, & [kg]; \\ I_b &= \sum_\beta m_\beta l_\beta^2 + \sum_\beta (F_{\beta 0} + F_{\beta 1}m + F_{\beta 2}v), & [kg \cdot m^2]; \quad \beta \in \{h, a_{1-3}, r_{1-3}\}, \end{aligned} \quad (1)$$

where constants  $k_\alpha$  define the position of the centres of gravity of a shank and a thigh in relation to the axes of rotation, see below. Constants  $l_\beta$  represent the distance of the centre of gravity of a respective upper body segment ( $h, a_{1-3}, r_{1-3}$ ) from the origin of coordinates ( $x_2, y_2$ ), see

Fig. 1. All these constants are specific for each individual or the respective movement pattern and thus it is essential to ascertain them from anthropomorphic measurements and a kinematic analysis. The values of parameters  $E, F$  are stated in Table 1.

**Tab. 1** Values of  $E, F$  parameters to determine the weight and moment of inertia of particular segments.

$\alpha$	$E_{\alpha 0}$ [kg]	$E_{\alpha 1}$ [ ]	$E_{\alpha 2}$ [cm <sup>-1</sup> ]	$F_{\alpha 0}$ [kg.cm <sup>2</sup> ]	$F_{\alpha 1}$ [cm <sup>2</sup> ]	$F_{\alpha 2}$ [kg.cm]
$s$	-1.59200	0.03616	0.01210	-1152.000	4.594	6.815
$t$	-2.64900	0.14630	0.01370	-3690.000	32.020	19.240
$\beta$	$E_{\beta 0}$ [kg]	$E_{\beta 1}$ [ ]	$E_{\beta 2}$ [cm <sup>-1</sup> ]	$F_{\beta 0}$ [kg.cm <sup>2</sup> ]	$F_{\beta 1}$ [cm <sup>2</sup> ]	$F_{\beta 2}$ [kg.cm]
$h$	0.64800	0.00855	0.00715	-56.000	0.715	0.865
$a_1$ (upper arm)	0.25000	0.03012	-0.00270	-232.000	1.526	1.343
$a_2$ (forearm)	0.31850	0.01445	-0.00114	-67.900	0.855	0.376
$a_3$ (hand)	-0.11650	0.00360	0.00175	-13.680	0.088	0.092
$r_1$ (upper)	4.10720	0.09310	-0.02920	183.500	9.150	-2.865
$r_2$ (medium)	3.59050	0.11170	-0.03315	131.500	13.350	-4.000
$r_3$ (nether)	-3.74900	0.04880	0.02448	467.000	5.900	1.720

Note: Parameters  $F$  are given for axes of rotation perpendicular to the sagittal body plane. The trunk  $r$  and the upper limb  $a$  are combined from three parts. With respect to the nature of the task, parameters  $E_\square$  and  $F_\square$  are specified so that  $m_b$  and  $I_b$  characterised the half of the upper body (i.e. only a half of the weight of the head, trunk and one hand are considered).

The model contains two links which anatomically represent an ankle joint and a knee joint. The third link is located in the pelvis area. The angle between the trunk and the thigh is maintained not only by the hip joint but also by the lumbar spine. Therefore, this link although located in the hip joint is not anatomically represented and only an approximation is concerned.

A coordinate system where the direction of the x-axis copies the direction of the previous segment is located in each joint. In total, three coordinate systems are involved. The angle between the x-axis and the next segment is described as  $q_1 - q_3$ . Angles formed by particular segments between themselves are described as  $\varphi_1 - \varphi_3$ . Relations between respective angles are as follows:

$$q_1 = \varphi_1; q_2 = \pi - \varphi_2; q_3 = \pi + \varphi_3. \quad (2)$$

Expressions (2) have particular practical importance. In theoretical analysis, it is advantageous to work with so called generalized coordinates  $q_i$  (see below), angles  $\varphi_i$  are used especially in experimental methods of biomechanics.

The centres of gravity of respective segments are described as follows. The total centre of gravity (COM) is determined by  $T$  in the picture,  $T_t$  represents the centre of gravity of a thigh,  $T_s$  is the centre of gravity of a shank. The centre of gravity of the upper body is represented by  $T_b$ . Positions of centres of gravity of particular segments are determined again in accordance with Zatsiorsky et al. [5]. In particular:

$$\begin{aligned} [x_1; y_1] &= k_s [L_s c_1; L_s s_1] \\ [x_2; y_2] &= [L_s c_1 + k_t L_t c_{12}; L_s s_1 + k_t L_t s_{12}] \\ [x_3; y_3] &= [L_s c_1 + L_t c_{12} + L_b c_{123}; L_s s_1 + L_t s_{12} + L_b s_{123}], \end{aligned} \quad (3)$$

where constants  $k_s = 6/10, k_t = 6/9, k_b = 1$  define the position of centres of gravity of respective segments with the length of  $L_t, L_s, L_b$  [m]. These must be ascertained for each individual. In the interest of clarity, the following marking is used in relations:

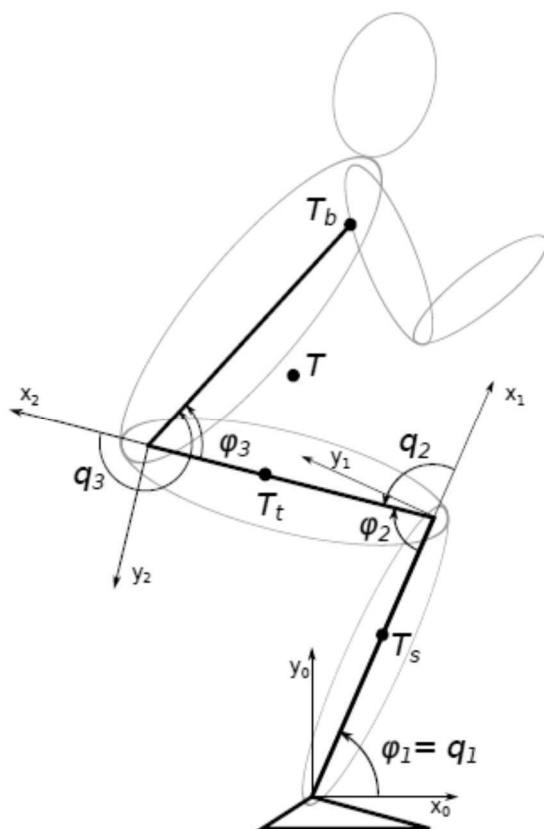


**Fig. 1** Stick model of the anthropomorphic mechanism

$$\begin{aligned} c_i &= \cos(q_i); & c_{ij} &= \cos(q_i + q_j); & c_{ijk} &= \cos(q_i + q_j + q_k); \\ s_i &= \sin(q_i); & s_{ij} &= \sin(q_i + q_j); & s_{ijk} &= \sin(q_i + q_j + q_k); \end{aligned} \quad i, j, k \in \{1, 2, 3\}. \quad (4)$$

With respect to the relations (1), it must be mentioned for the sake of completeness that the positions of the centres of gravity of respective segments of the upper body are located close to the hand and the trunk in 4/10 of their total length. In case of the upper arm and the forearm it is represented by 4/9 taken from the proximal end of the segment (i.e. closer to the body centre) [5]. In case of the head with the throat (taken as one segment), the centre of gravity is located in 1/2 of the total length.

### 3 Form of motion equations

$$\begin{aligned} E_k &= \frac{1}{2} \left( m_s (\dot{x}_1^2 + \dot{y}_1^2) + m_t (\dot{x}_2^2 + \dot{y}_2^2) + m_b (\dot{x}_3^2 + \dot{y}_3^2) + I_s \dot{q}_1^2 + I_t (\dot{q}_1 + \dot{q}_2)^2 + I_b (\dot{q}_1 + \dot{q}_2 + \dot{q}_3)^2 \right) \\ E_p &= m_s g y_1 + m_t g y_2 + m_b g y_3 \end{aligned} \quad (6)$$

The resulting form of motion equations may be described in a matrix form:

$$B(q)\ddot{q} + C(q; \dot{q})\dot{q} + g(q) = Q, \quad (7)$$

where  $B$  represents the so-called weight matrix,  $C$  is a velocity matrix,  $g$  is a vector of gravitational forces,  $q$  is a

$$\begin{pmatrix} b_{11} & b_{12} & b_{13} \\ b_{21} & b_{22} & b_{23} \\ b_{31} & b_{32} & b_{33} \end{pmatrix} \begin{pmatrix} \ddot{q}_1 \\ \ddot{q}_2 \\ \ddot{q}_3 \end{pmatrix} + \begin{pmatrix} c_{11} & c_{12} & c_{13} \\ c_{21} & c_{22} & c_{23} \\ c_{31} & c_{32} & c_{33} \end{pmatrix} \begin{pmatrix} \dot{q}_1 \\ \dot{q}_2 \\ \dot{q}_3 \end{pmatrix} + \begin{pmatrix} g_1 \\ g_2 \\ g_3 \end{pmatrix} = \begin{pmatrix} Q_1 \\ Q_2 \\ Q_3 \end{pmatrix}, \quad (8)$$

where:

$$\begin{aligned} b_{11} &= m_s k_s^2 L_s^2 + m_t L_s^2 + m_t k_t^2 L_t^2 + m_b (L_s^2 + L_t^2 + L_b^2) + 2(m_t k_t L_s L_t + m_b L_s L_t) c_2 + 2m_b L_b L_t c_3 + 2m_b L_s L_b c_{23} + I_s + I_t + I_b \\ b_{12} &= m_t k_t^2 L_t^2 + m_b (L_t^2 + L_b^2) + (m_t k_t L_s L_t + m_b L_s L_t) c_2 + 2m_b L_b L_t c_3 + m_b L_s L_b c_{23} + I_t + I_b = b_{21} \\ b_{13} &= m_b L_b^2 + m_b L_b L_t c_3 + m_b L_s L_b c_{23} + I_b = b_{31} \\ b_{22} &= m_t k_t^2 L_t^2 + m_b (L_t^2 + L_b^2) + 2m_b L_t L_b c_3 + I_t + I_b \\ b_{23} &= m_b L_b^2 + m_b L_t L_b c_3 + I_b = b_{32} \\ b_{33} &= m_b L_b^2 + I_b \\ c_{11} &= -2(m_t k_t L_s L_t + m_b L_s L_t) s_2 \dot{q}_2 - 2m_b L_b L_t s_3 \dot{q}_3 - 2m_b L_b L_s s_{23} (\dot{q}_2 + \dot{q}_3) \\ c_{12} &= -(m_t k_t L_s L_t + m_b L_s L_t) s_2 \dot{q}_2 - 2m_b L_b L_t s_3 \dot{q}_3 - m_b L_b L_s s_{23} (\dot{q}_2 + \dot{q}_3) \\ c_{13} &= -m_b L_b L_t s_3 \dot{q}_3 - m_b L_b L_s s_{23} (\dot{q}_2 + \dot{q}_3) \\ c_{21} &= (m_t k_t L_s L_t + m_b L_s L_t) s_2 \dot{q}_1 - 2m_b L_b L_t s_3 \dot{q}_3 - m_b L_b L_s s_{23} (\dot{q}_2 + \dot{q}_3) \\ c_{22} &= -2m_b L_t L_b s_3 \dot{q}_3 \\ c_{23} &= -m_b L_b L_t s_3 \dot{q}_3 + m_b L_s L_t s_{23} \dot{q}_1 \\ c_{31} &= m_b L_b L_t s_3 (\dot{q}_1 + 2\dot{q}_2) + m_b L_b L_s s_{23} \dot{q}_1 \\ c_{32} &= m_b L_b L_t s_3 \dot{q}_2 \\ c_{33} &= 0 \\ g_1 &= m_s g k_s L_s c_1 + m_t g (L_s c_1 + L_t k_t c_{12}) + m_b g (L_s c_1 + L_t c_{12} + L_b c_{123}) \\ g_2 &= m_t g k_t L_t c_{12} + m_b g (L_t c_{12} + L_b c_{123}) \\ g_3 &= m_b g L_b c_{123} \end{aligned}$$

The equation (7), or (8) as the case may be, are signifi-

cantly simplified if the so-called quasi-static approximation is considered. Assuming the whole motion of the

$$\frac{d}{dt} \left( \frac{\partial E_k}{\partial \dot{q}_i} \right) - \frac{\partial E_k}{\partial q_i} + \frac{\partial E_p}{\partial q_i} = Q_i, \quad (5)$$

where  $E_k$  represents the total kinetic energy and  $E_p$  the total potential energy of the system. It is established as follows:

vector of independent generalized coordinates (for the angles in this model, see above) and  $Q$  are generalized forces (moments of inertia in this model). A specific solution is as follows:

cantly simplified if the so-called quasi-static approximation is considered. Assuming the whole motion of the

mechanism is very slow. In such a case, the first two equation members may be omitted and the following is established:

$$g(q) = Q. \quad (9)$$

This approach may be used to diagnose the lifting of patients from sitting to standing [6] or during a permanently lowered posture (e.g. downhill posture).

#### 4 Model application example (quasi-static approximation)

Now an example of a model application follows in its quasi-static approximation. For this purpose, a five-stage kinematogram of a deep squat of a proband with the body weight  $m = 55$  kg and body height  $v = 165$  cm was created, see Fig 2.

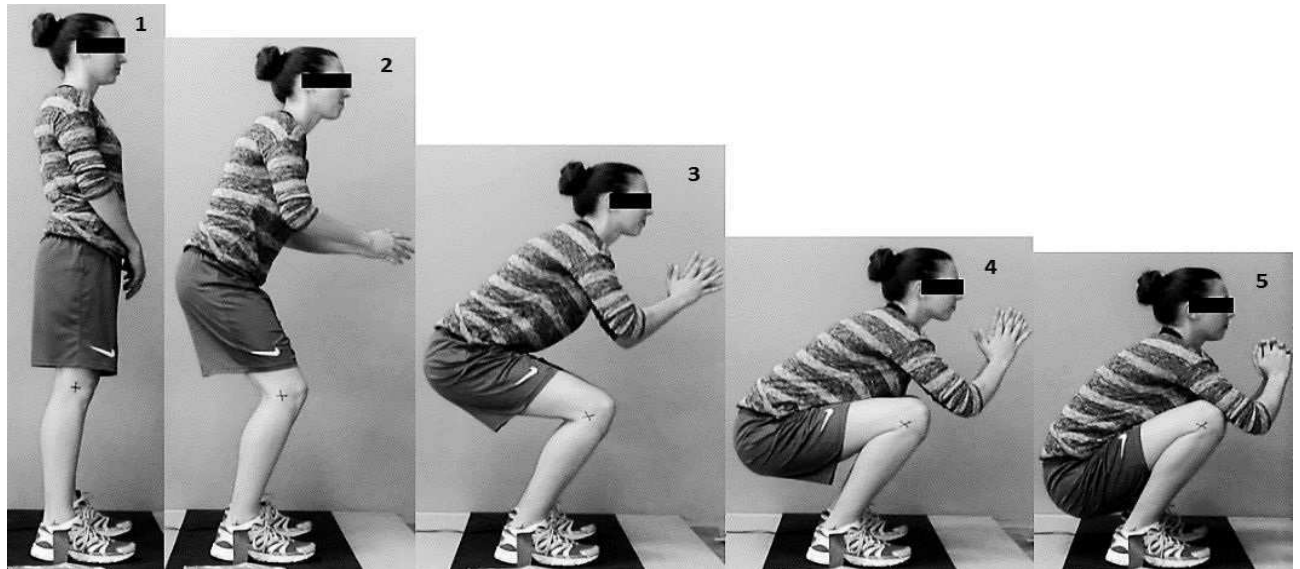


Fig. 2 Kinematogram of deep squat (Positions 1-5)

A stick model of an anthropomorphic mechanism according to Fig. 1 was added to each position. Furthermore, respective values of angles  $\varphi_1 - \varphi_3$  were deduced

and resulting moments of forces in a particular joint were determined by means of derived equations (9). Their dependence on partial positions of the deep squat is depicted in Fig. 3.

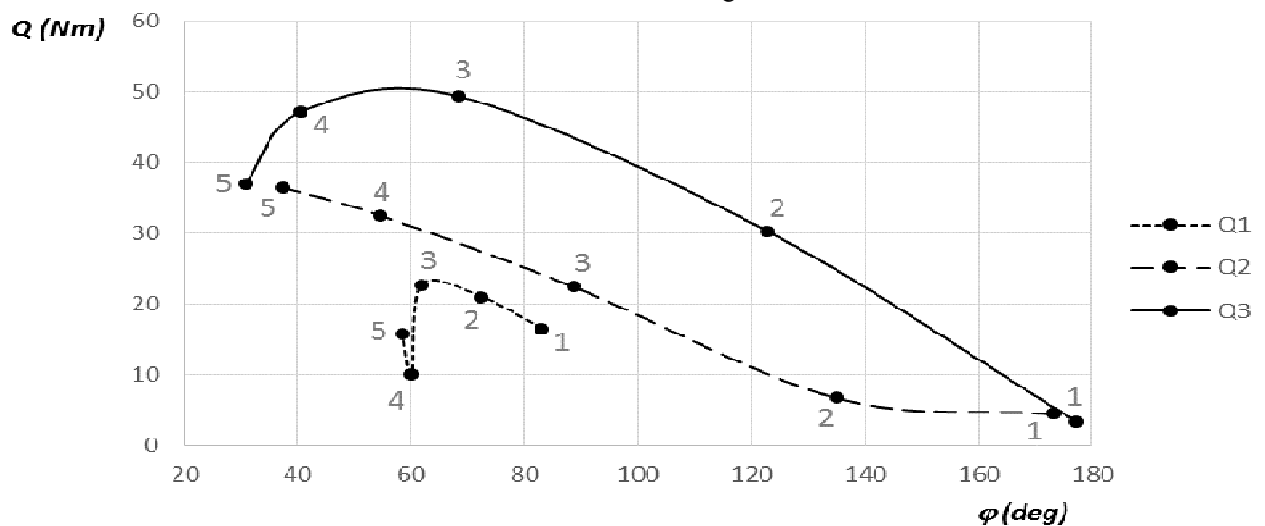


Fig. 3 Graph showing the dependence of moments of forces on the angle of flexion in a respective joint link  
Legend: Q1 – ankle joint, Q2 – knee joint, Q3 – hip joint  
Numbers 1-5 correspond with respective positions according to Fig. 2

The results depicted in the graph of Fig. 3 may, among other things, be used for the following conclusions. When moving from a deep squat to a stand (Positions 5-1):

1. The moment of force in the area of a hip joint reaches its maximum between Pos. 3 and 4, i.e. in the moment when the flexion in the knee corresponds to approximately  $90^\circ$ . This moment of

force continually decreases from Pos. 3 to Pos. 1.

2. The moment of force in the knee joint necessary for its extension decreases.

3. The moment of force in the ankle joint reaches its maximum in Pos. 3.

## 5 Discussion

The model has certain limitations in its application. One of the drawbacks is the precision in determining the geometry from the stick model. Selection of the experimental method which will provide data inputs for equations (7) is essential here. The experience gained so far shows that satisfying results may be reached by combining 3D kinematic analysis (e.g. Qualisys system) with dynamographical systems (e.g. EMED strain-gauge platform). The combination of these experimental methods may be used to calibrate the model by means of the relation of COM and COP using the findings of Morasso et al. [7].

Furthermore, it is necessary to realize that the sizes of moments in particular joint links represent only approximate estimations. The model respects neither the precise anatomic alignment of respective joints nor related muscle groups (it is known, for example, that the femoral head performs a rotational sliding motion against tibia during flexion in the knee joint).

Nevertheless, in connection with a suitable anatomic and kinesiologic analysis, the whole approach contributes significantly especially in the context of selected functional and structural disorders of the musculoskeletal system. But for these purposes, the model must be locally (in a respective joint link) extended by the above mentioned anatomic aspects. The application of clinic CT image data is also assumed, e.g. see [8], [9]. Information about the moment effects in the knee and ankle joints may further be used to simulate the pressure distribution, e.g. see [10] inside these joint links.

## 6 Conclusion

The presented model of an anthropomorphic mechanism enables supplementing the common kinematic analysis of a deep squat with estimations of resulting moments of forces applied to the main joints of the bottom body part. The results gained herein may be used for a complex biomechanical analysis of this movement pattern and also for the analysis of related forms of movement with similar geometry (e.g. standing-up, squatting with a dumbbell, skiing in downhill posture, two-footed jump, etc.).

The following research will focus on the extension of the model by dissipative processes in particular joints, inclusion of local anatomic aspects and furthermore by its verification. The aim is to apply the whole technology during studies of selected disorders of the musculoskeletal system of a human.

## Acknowledgement

**This project was supported by grants PROGRES Q41 and TG01010117 – PROSYKO**

## References

- [1] BLOOMQUIST, K., et al. (2013). Effect of range of motion in heavy load squatting on muscle and tendon adaptations. *European Journal of applied physiology*. 2013, 113(8), 2133-42. ISSN 1430-6319.
- [2] BRYANTON, Megan A., et al. (2012). Effect of squat depth and barbell load on relative muscular effort in squatting. *Journal of Strength and Conditioning Research*. 2012, 26(10), 2820-8. ISSN 1064-8011.
- [3] ESFORMES, Joseph I. a Theodoros M. BAMPOURAS. (2013). Effect of back squat depth on lower-body postactivation potentiation. *Journal of Strength and Conditioning Research*. 2013, 27(11), 2997-3000. ISSN 1064-8011.
- [4] HARTMANN, Hagen, et al. (2012). Influence of squatting depth on jumping performance. *Journal of Strength and Conditioning Research*. 2012, 26(12), 3243-63. ISSN 1064-8011.
- [5] ZACIORSKI, V. M., ARUIN, A. S., & SELUJANOV, V. N. (1981). *Biomechanics of the locomotor apparatus of man*. 1981. Moskva: FiS.
- [6] RAVNIK, D., VRANÝ, J., JELEN, K., BITTNER, V. (2017). Biomechanical Aspects of Assisting Patients in Standing up in the Context of Ergonomics. ZUNJIC, Aleksandar. *Ergonomic Design and Assessment of Products and Systems*. 2017. New York: Nova Science Publishers, s. 19. ISBN 978-1-53611-784-4.
- [7] MORASSO, Pietro G., Gino SPADA a Roberto CAPRA. (1999). Computing the COM from the COP in postural sway movements. *Human Movement Science*. 1999, 18(6), 759-767. DOI: 10.1016/S0167-9457(99)00039-1. ISSN 01679457.
- [8] SEDLAK, J., CHLADIL, J., SLANY, M., KOURIL, K. (2014). Introduction to processing of CT clinical metadata of disabled part of patient knee joint. *Manufacturing Technology*. 2014, 14(4), pp. 611-618.
- [9] SEDLAK, J., SLANY, M., FIALA, Z., JAROS, A. Production method of implant prototype of knee-joint femoral component. *Manufacturing Technology*; 2015; 15(2), pp. 195-204
- [10] VAVRO, J., VAVRO, J., KOVÁČIKOVÁ, P., BEZDEDOVÁ, R., HÍŘEŠ, (2017). Kinematic and dynamic analysis and distribution of stress in items of planar mechanisms by means of the MSC ADAMS software. *Manufacturing Technology*. 2017, 17(3), pp. 397-401.